pler, *Immunity* **3**, 187 (1995).
7. Covalent complexes of I-E^k–Hb and I-E^k–Hsp were produced as soluble heterodimers in insect cells with a baculovirus expression system (*5, 6*). Secreted class II molecules were immunopurified from culture supernatants with the I-E^k antibody 14-4-4, followed by size exclusion chromatography with Superdex-200 (Pharmacia).
8. We grew crystals of I-E^k–Hb and I-E^k–Hsp of data collection quality by equilibrating 5 to 10 mg/ml of purified protein against 16 to 18% polyethylene glycol 4000 (Fluka), 2% ethylene glycol, 200 mM ammonium sulfate, and 100 mM citrate (pH 5.2 to 5.6). Crystals were cryoprotected by the addition of 20% polyethylene glycol 4000, 20% ethylene glycol, and 10% glycerol.
9. B. D. Evavold, S. G. Williams, B. L. Hsu, S. Buus, P. M. Allen, *J. Immunol.* **148**, 347 (1992).
10. P. Marrack, L. Ignatowicz, J. W. Kappler, J. Boymel, J. H. Freed, *J. Exp. Med.* **178**, 2173 (1993).
11. Crystals were cryopreserved in a −160°C nitrogen stream, and data were collected at the HHMI X-4A beamline of the National Synchrotron Light Source at Brookhaven National Laboratory. For I-E^k–Hb, data were measured from two crystals at wavelengths of 0.9879 Å and 1.0070 Å, whereas x-rays of 0.9789 Å wavelength were used on a single crystal of I-E^k–Hsp. Data were collected on Fuji imaging plates for 2 to 4 min with 2° oscillation ranges. These data were autoindexed and processed with DENZO [Z. Otwinowski, L. Sawyer, N. Isaacs, S. Bailey, Eds. (SERC Daresbury Laboratory, Warrington, UK, 1993), pp. 56], scaled with SCALA, and merged with AGROVATA (SERC Collaborative Computing Project No. 4, Daresbury Laboratory, Warrington, UK, 1979). The I-E^k–Hb crystals belong to space group *C*2 with unit cell dimensions a = 147.0 Å, b = 57.1 Å, c = 117.0 Å, and β = 91.5°. A total of 169,034 observations were merged to 38,809 reflections with an R_{sym} = 0.075 and 89.2% completion between 20 and 2.3 Å. $R_{sym} = \Sigma|I - \langle I \rangle|/\Sigma I$, where I is the observed intensity and $\langle I \rangle$ is the average intensity obtained from multiple observations of symmetry-related reflections. The I-E^k–Hsp crystals belong to space group P3,21 with unit cell dimensions $a = b$ = 77.6 Å and c = 319.6 Å. A total of 85,623 observations were merged to 29,069 reflections with an R_{sym} = 0.087 and 92.1% completion between 20 and 2.7 Å. The solvent contents are 55% and 60% for the respective crystals with two heterodimeric complexes per asymmetric unit.
12. Phases for the I-E^k–Hb data were obtained by molecular replacement with the coordinates of a single HLA-DR1 heterodimer (*15*) with mismatched amino acid residues replaced with Ala side chains. AMORE [J. Navaza, *Acta Crystallogr.* **50**, 157 (1994)] rotation and translation function results were unambiguous for two heterodimers in the asymmetric unit. The molecular replacement structure of I-E^k–Hsp was solved with a single heterodimer of the partially refined I-E^k–Hb. After rigid body refinement, the R factors for I-E^k–Hb and I-E^k–Hsp were 43% and 37%, respectively, for data from 8 to 3 Å.
13. Model building was carried out with a modified version of TOM/FRODO [T. A. Jones, *J. Appl. Crystallogr.* **11**, 268 (1978)]. Minimization and simulated annealing refinements were carried out with X-PLOR [A. Brunger, X-PLOR, version 3.1 manual (Yale Univ. Press, New Haven, 1992)], which used noncrystallographic symmetry restraints. For I-E^k–Hb, the current model for each half of the dimer contains 182 residues of I-Eα^d (α1 to α182), 13 mouse Hb(64–76) residues (P-4 to P9), 16 linker residues (P+1 to P+16) connecting to 185 residues of the natural I-Eβ^k (β^4 to β^{188}), and 3 carbohydrates N-linked to Asn$^{\alpha 78}$, Asn$^{\alpha 118}$, and Asn$^{\beta 19}$. There are 349 water molecules in the dimer for a total of 6773 nonhydrogen atoms. The R value stands at 21.1% for all data from 6 to 2.3 Å with an R_{free} of 28.5% (for data greater than 2σ, R = 20.8% and R_{free} = 28.2%). The average atomic temperature factor is 32.3 Å^2, and the model has root-mean-square (rms) deviations of 0.010 Å and 1.63° from ideal bond lengths and angles, respectively. The I-E^k–Hb complexes can be superimposed with an rms deviation of 0.35 Å. For I-E^k–Hsp, the current model for each complex contains 182 residues of I-Eα^d (α1 to α182), 2 residues NH_2-terminal to the peptide (P-4 to P-3), 13 mouse Hsp70 (236 to 248) residues (P-2 to P+2), 14 linker residues (P+3 to P+16) connecting to 185 residues of the natural I-Eβ^k (β4 to β188), and 3 carbohydrates. There are 159 water molecules and 1 sulfate ion for a total of 6676 nonhydrogen atoms. The R value stands at 23.3% for all data from 6 to 2.3 Å with an R_{free} value of 33.4% (for data greater than 2σ, the R = 22.2% and R_{free} = 32.1%), with an average temperature factor of 36.5 Å^2 and rms deviations of 0.011 Å and 1.73° from ideal bond lengths and angles, respectively. The two I-E^k–Hsp complexes compare favorably with an rms deviation of 0.37 Å. For both models, no attempt was made to build the peptide NH_2-terminal regions (P-8 to P-5 of Hb and P-7 to P-5 of Hsp) or the COOH-terminal 10 residues of either the α or β chains, as these regions appear highly disordered in the electron density maps. The density for residues β107 to β113 was poor in both peptide complexes; this segment is modeled as polyalanine.
14. L. Ignatowicz, G. Winslow, J. Bill, J. Kappler, P. Marrack, *J. Immunol.* **154**, 3852 (1995).
15. L. J. Stern *et al.*, *Nature* **368**, 215 (1994).
16. P. Ghosh, M. Amaya, E. Mellins, D. C. Wiley, *ibid.* **378**, 457 (1995).
17. J. H. Brown *et al.*, *ibid.* **364**, 33 (1993).
18. T. S. Jardetzky *et al.*, *ibid.* **368**, 711 (1994).
19. P. A. Reay, R. M. Kantor, M. M. Davis, *J Immunol.* **152**, 3946 (1994).
20. H. Schild *et al.*, *Int. Immunol.* **7**, 1957 (1995).
21. J. L. Jorgensen, U. Esser, B. F. de St. Groth, P. A. Reay, M. M. Davis, *Nature* **355**, 224 (1992).
22. B. D. Evavold and P. M. Allen, *Science* **252**,. 1308 (1991); B. D. Evavold, J. Sloan-Lancaster, B. L. Hsu, P. M. Allen, *J. Immunol.* **150**, 3131 (1993); L. M. Spain, J. L. Jorgensen, M. M. Davis, L. J. Berg, *ibid.* **152**, 1709 (1994).
23. D. H. Fremont *et al.*, *Proc. Natl. Acad. Sci. U.S.A.* **92**, 2479 (1995).
24. P. E. Jensen, *J. Exp. Med.* **171**, 1779 (1990); A. Sette *et al.*, *J. Immunol.* **148**, 844 (1992); J. Boniface *et al.*, *Biochemistry* **32**, 11761 (1993); P. Reay, D. Wettstein, M. M. Davis, *EMBO J.* **11**, 2829 (1992).
25. Nir Ben-Tal , D. H. Fremont, A. Windemuth, W. A. Hendrickson, B. Honig, unpublished results. The pK_a is the negative logarithm of the acid constant.
26. M. Carson, *J. Mol. Graphics* **5**, 103 (1987).
27. M. L. Connolly, *ibid.* **3**, 19 (1985). Solvent-accessible surface calculations were performed with a 1.4 Å probe sphere.
28. The following residues make at least one contact (≤4.0 Å) in either the I-E^k–Hb or I-E^k–Hsp dimer interface: Lys$^{\alpha 2}$, Glu$^{\alpha 4}$, Asp$^{\alpha 141}$, Tyr$^{\beta 18}$, Arg$^{\beta 23}$, Arg$^{\beta 25}$, Arg$^{\beta 39}$, Asp$^{\beta 41}$, Asp$^{\beta 43}$, Val$^{\beta 44}$, Arg$^{\beta 48}$, Val$^{\beta 50}$, Glu$^{\beta 52}$, Arg$^{\beta 55}$, Lys$^{\beta 139}$, Thr$^{\beta 140}$, Gly$^{\beta 141}$, Ile$^{\beta 142}$, Val$^{\beta 143}$, Ser$^{\beta 144}$, Thr$^{\beta 145}$, Gly$^{\beta 146}$, Leu$^{\beta 147}$, Met$^{\beta 160}$, and the peptide linker residues Gly^{P+3}, Gly^{P+4}, Ser^{P+5}, Leu^{P+6}, and Val^{P+7}. In only the I-E^k–Hsp dimer is a sulfate ion found coincident with the noncrystallographic diad axis sequestered by four Arg residues (Arg$^{\beta 25}$ and Arg$^{\beta 29}$). There is no obvious reason why a sulfate ion is not also present in the I-E^k–Hb crystal. Perhaps dimer packing in the different space groups, slight differences in pH, or small changes in the dimer interface controlled the sequestering of the sulfate ion. There is no obvious influence of the peptide or linker on sulfate coordination.
29. We thank J. Clements, F. Crawford, H. Kozono, D. Parker, and J. White for help in making the soluble class II molecules and H.-E. Aronson, K. Choi, C. Lima, X. Zhao, and X. Zhu for aid in the synchrotron data collection and Nir Ben-Tal for electrostatic discussions. Coordinates have been deposited in the Brookhaven Protein Data Bank (entries 1IEA and 1IEB) and are available via e-mail (fremont@columbia.edu).

14 November 1995; accepted 1 March 1996

Specification of Pituitary Cell Lineages by the LIM Homeobox Gene *Lhx3*

Hui Z. Sheng,* Alexander B. Zhadanov,*† Bedrich Mosinger Jr.,‡ Tetsuya Fujii,§ Stefano Bertuzzi,‖ Alexander Grinberg, Eric J. Lee, Sing-Ping Huang, Kathleen A. Mahon,¶ Heiner Westphal¶#

During pituitary organogenesis, the progressive differentiation of distinct pituitary-specific cell lineages from a common primordium involves a series of developmental decisions and inductive interactions. Targeted gene disruption in mice showed that *Lhx3*, a LIM homeobox gene expressed in the pituitary throughout development, is essential for differentiation and proliferation of pituitary cell lineages. In mice homozygous for the *Lhx3* mutation, Rathke's pouch formed but failed to grow and differentiate; such mice lacked both the anterior and intermediate lobes of the pituitary. The determination of all pituitary cell lineages, except the corticotrophs, was affected, suggesting that a distinct, *Lhx3*-independent ontogenetic pathway exists for the initial specification of this lineage.

Pituitary organ commitment occurs during the formation of Rathke's pouch, the ectodermal primordium of the anterior and intermediate lobes of the pituitary, when it comes in contact with neuroectoderm of the ventral hypothalamus (*1*). Inductive interactions between these tissues are required for their proper determination and differentiation (*2–5*). Once committed to the pituitary fate, the epithelium lining Rathke's pouch proliferates and differentiates into pituitary-specific cell lineages that secrete peptide hormones critical for homeostasis, growth, and reproduction (*6, 7*). The mouse LIM homeobox gene *Lhx3* (also known as *mLim-3* and *P-Lim*) (*8–10*) and its *Xenopus* counterpart *Xlim3* (*11*) are expressed in the pituitary throughout development and in the adult. *Lhx3* is also expressed in the developing hindbrain, spinal cord, and pineal gland.

To analyze the function of *Lhx3*, we

created an *Lhx3*$^{-/-}$ mutant mouse by deleting part of the gene encoding the two LIM domains and some of the homeodomain (Fig. 1, A and B). In situ hybridization with an *Lhx3*-specific probe confirmed that *Lhx3* transcripts were missing in mutant embryos (*12*). Mice heterozygous for the *Lhx3* mutation were apparently normal and fertile, but homozygous embryos were either stillborn or died within 24 hours after birth. Those that survived birth were of normal size and color and were indistinguishable from their wild-type siblings in their ability to breathe, suckle, and move. The exact cause of death has not been determined but may result from deficits in brain stem function because *Lhx3* is expressed in the putative precursor cells of the Raphe nuclei and part of the reticular formation (*10*). Although the hindbrain, spinal cord, and pineal gland were grossly normal, the *Lhx3* mutant lacked the anterior and intermediate lobes of the pituitary. The posterior lobe of the pituitary appeared grossly normal (Fig. 2, A and E). These mice also had hypoplastic adrenal cortexes, secondary to pituitary hormone deficits, which suggests that lack of glucocorticoids was a contributing factor in their failure to survive. However, other mouse models of adrenal insufficiency typically survive longer (*13*), and dexamethasone supplementation failed to rescue *Lhx3* mutant neonates (*12*), which argues against adrenal insufficiency as the exclusive cause of death.

Histological analysis of mutant embryos showed that Rathke's pouch was initially formed in −/− embryos but failed to grow (Fig. 2). At embryonic day (E) 10.5, Rathke's pouch in −/− embryos resembled the wild-type pouch (Fig. 2B), except that its opening to the oral cavity was consistently wider and the epithelial cells lining the pouch were multilayered and appeared less columnar (Fig. 2F), suggesting that the pouch did not invaginate as far as normal. By E12.5, the wall of Rathke's pouch in the wild-type mouse was thickened and the connection between the pouch and the oral cavity was lost (Fig. 2C). In contrast, the wall of the −/− pouch remained a thin layer of epithelium, retaining a connection, albeit narrowed, to the oral cavity (Fig. 2G). By E15.5, the wild-type pouch had developed into a gland with distinct cell types (Fig. 2D), whereas the −/− pouch remained a thin layer of epithelium connected to the oral cavity (Fig. 2H). Tunel staining revealed that the growth arrest was due to a failure in proliferation as opposed to increased apoptosis (*12*).

The growth arrest of Rathke's pouch was accompanied by changes in the expression of pituitary-specific marker genes (Fig. 3). The *Rpx* homeobox gene is expressed very early in pituitary ontogeny in the anterior neural plate and in Rathke's pouch, from its initial formation to E14.5, when expression is extinguished coincident with the differentiation of pituitary cell types (*14*). At E10.5, we detected *Rpx* transcripts in the pouch epithelium in both the wild-type and *Lhx3*$^{-/-}$ mice, which suggests that the initial specification of the pouch had occurred normally (Fig. 3A). At E12.5, *Rpx* expression continued in the wild-type pituitary but had ceased in the *Lhx3*$^{-/-}$ pouch (Fig. 3B). Thus, the initial expression of *Rpx* in the pouch is independent of *Lhx3* protein, whereas continued expression after 10.5 days is either directly or indirectly dependent on *Lhx3*. The loss of *Rpx* expression heralds the first detectable alteration in the developmental program of the primordial pituitary cells and establishes the time between E10.5 and E12.5 as a critical period for *Lhx3* gene function in pituitary organogenesis. This early change presum-

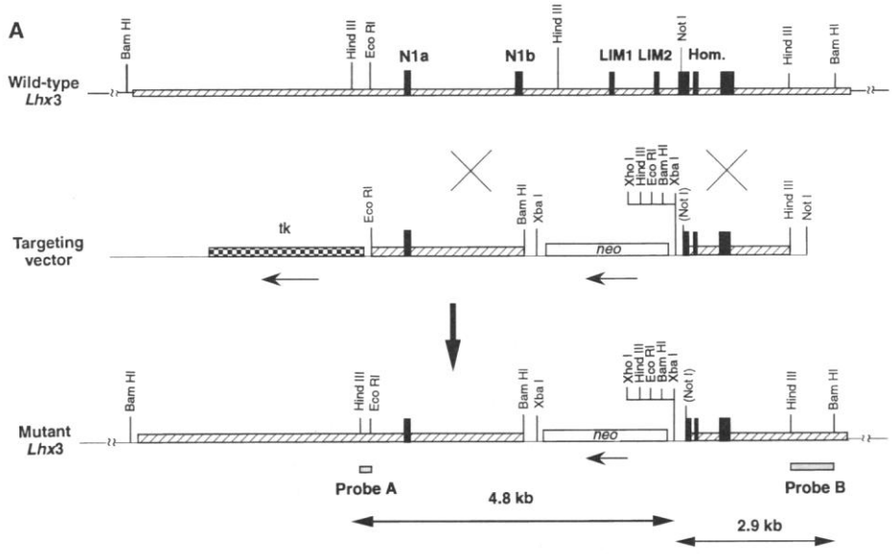

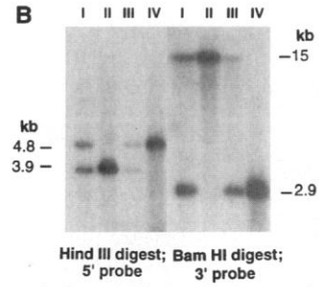

Fig. 1. (**A**) Targeting of the *Lhx3* gene by homologous recombination in embryonic stem cells. Diagrammatic representation of the wild-type *Lhx3* locus, the targeting vector, and the *Lhx3* mutant locus after targeting. The two NH_2-termini of *Lhx3* are indicated by N1a and N1b. LIM1, LIM domain 1; LIM2, LIM domain 2; hom., homeodomain (*21*). Expected sizes of the wild-type and mutant fragments were 3.9 and 4.8 kb, respectively, for the Hind III digest and 15 and 2.9 kb, respectively, for the Bam HI digest. (**B**) Southern (DNA) blot showing correct targeting of the *Lhx3* locus and genotyping of progeny. DNA samples derived from targeted embryonic stem (ES) cells (I) and from tails of the wild-type (II), heterozygous (III), and homozygous (IV) mice were digested with restriction enzymes and probed with 5′ and 3′ probes as indicated. Murine *Lhx3* genomic clones were isolated from the EMBL3A 129/J1 mouse genomic library (*21*) with the use of a cDNA probe including the 5′ untranslated region of the *Lhx3b* transcript and 70% of the coding sequence for screening. A double-selection replacement vector was constructed in pPNT (*22*), substituting the 5′ terminal region of *Lhx3* gene, including the region encoding the LIM domains and part of the homeodomain, with a neomycin-resistance (*neo*) gene flanked by 2.4 kb (5′) and 2.1 kb (3′) of homologous sequence and the thymidine kinase (tk) gene. The vector was linearized with Not I and electroporated into J1 line ES cells (*23*). One hundred twenty-three clones resistant to double selection (with G418, 350 mg/ml; and with gancyclovir, 2 mM) were screened by Southern blot hybridization with probes A and B. Seven clones were identified as correctly targeted. Chimeric mice were produced by either blastocyst injection (*22*) or by aggregation (*24*). Genotyping of embryos at late gestation that were derived from the intercross of heterozygotes (E16.5 to E18.5) showed the expected frequency of genotypes (24.4% −/−, 23.6% +/+, and 51.97% +/−; n = 127). Homozygous progeny derived from two independent clones (LB and Z64) had the same phenotype.

Laboratory of Mammalian Genes and Development, National Institute of Child Health and Human Development, National Institutes of Health, Bethesda, MD 20892, USA.

*Co–first authors.
†Present address: Department of Microbiology and Immunology, Jefferson Cancer Institute, Thomas Jefferson University, Philadelphia, PA 19107, USA.
‡Present address: Laboratory of Molecular Genetics, Institute for Mother and Child Care, 14710 Prague 4, Czech Republic.
§Present address: Department of Obstetrics and Gynecology, Asahikawa Medical College, Nishikagura 4-5, Hokkaido, 078, Japan.
‖On leave from Instituto di Microbiologia, Università Cattolica, Milan, Italy.
¶Co–senior authors.
≠To whom correspondence should be addressed at Laboratory of Mammalian Genes and Development, NICHD, NIH, Building 6B, Room 413, Bethesda, MD 20892–2790, USA.

ably presages the general arrest of the growth and differentiation of the pouch that is seen at later stages.

Pituitary development in mutant embryos was further assessed by the analysis of a variety of pituitary-specific lineage markers. The gene encoding the α-glycoprotein subunit (αGSU), the common component of the heterodimeric thyroid-stimulating hormone (TSH), luteinizing hormone (LH), and follicle-stimulating hormone (FSH), is the first hormone gene to be activated in the pituitary. The activation of the other peptide hormone genes follows that of the αGSU gene and occurs in a specific order during pituitary ontogeny (*6*, *15*, *16*). The transcription factor *Pit-1* directly regulates the genes encoding the β subunit of TSH (βTSH), growth hormone (GH), and prolactin (PRL) in vitro, and also helps to specify and maintain the thyrotroph, somatotroph, and lactotroph cell lineages (*7*). *Lhx3* binds and activates the promoter of αGSU and synergizes with *Pit-1* in the ac-

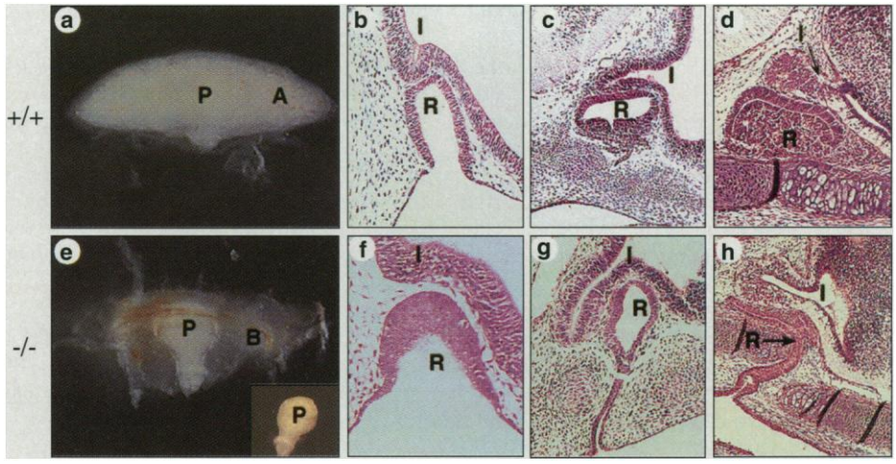

Fig. 2. Morphological and histological analysis of pituitary development in the wild-type (**a** through **d**) and *Lhx3*$^{-/-}$ mice (**e** through **h**). (a and e) Pituitary glands dissected from newborn mice. (a) Normal pituitary. (e) A −/− mutant pituitary, still wrapped in the bursa. The posterior lobe in the −/− mutant is grossly normal and is seen dissected free of the bursa in the inset; both the anterior and intermediate lobes are absent [confirmed by histological analysis (*12*)]. Red streaks in (a) and (e) are blood vessels. Sections of (b) wild-type and (f) mutant Rathke's pouches at E10.5. The epithelium of the −/− pouch appears multilayered. (c and g) Rathke's pouches at E12.5 and (d and h) E15.5. Arrest of growth and differentiation is apparent in E12.5 (g) and E15.5 (h) −/− mutant pouches. Although the ventral aspect of the wild-type pouch has proliferated to form the anterior lobe, the −/− pouch remains as a thin layer of epithelium with an open lumen to the oral cavity, a configuration reminiscent of earlier stages of pouch development. A, anterior lobe; P, posterior lobe; B, bursa; R, Rathke's pouch; and I, infundibulum. Preparation was as follows: Embryos were collected in phosphate-buffered saline. Either the yolk sac or tail was removed for genotyping, and the embryos were fixed in 4% paraformaldehyde at 4°C. Samples were dehydrated, embedded in paraffin, sectioned at 5 μm, and processed for hematoxylin and eosin staining.

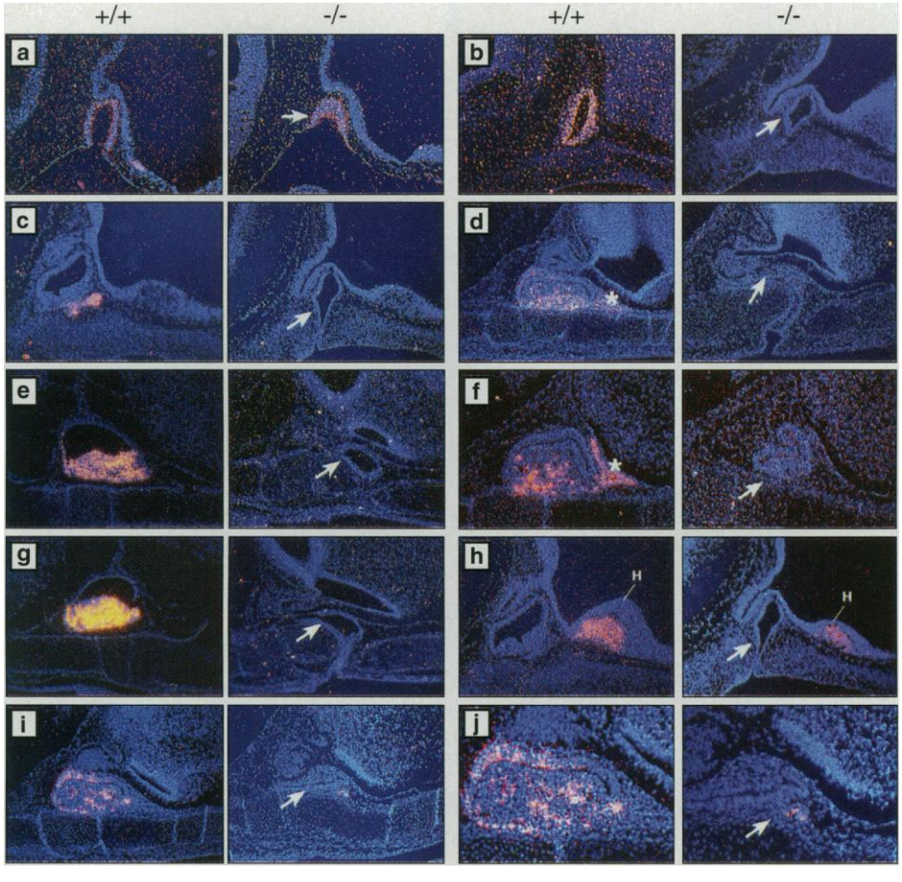

Fig. 3. Expression of pituitary marker genes in *Lhx3*$^{-/-}$ embryos. In situ hybridization of sections of Rathke's pouch from wild-type (left panels) and *Lhx3*$^{-/-}$ embryos (right panels). *Rpx* was expressed in wild-type Rathke's pouch at both E10.5 (**a**) and E12.5 (**b**), whereas its expression in the −/− pouch was on at E10.5 (a) but off at E12.5 (b). αGSU transcripts were detected in the wild-type animal at E12.5 (**c**) and E15.5 (**d**). αGSU expression was absent in the −/− pouch in both time points. *Pit-1* (**e**), βTSH (**f**), and GH (**g**) transcripts were detected in the E15.5 (e) or E16.5 (f and g) wild-type pituitary and were absent in the −/− pouch (e through g). At E12.5, POMC expression was detected only in the floor of the diencephalon but not in the pouch of either the wild-type or mutant pituitary (**h**). At E15.5, strong POMC expression appears in numerous cells in both the anterior and intermediate lobes of the wild-type pituitary (**i** and **j**). However, only a few POMC^{+} corticotroph cells were seen in the ventral base of the pouch remnant in the −/− mutant (I), which can be seen more clearly at higher magnification (j). White arrows indicate Rathke's pouches in mutants. Asterisks in (d) and (f) indicate the rostral tip. The hypothalamus in (h) is indicated by a capital H. Preparation was as follows: Sagittal sections of wax-embedded embryos were hybridized to ^{33}P-labeled riboprobes specific to αGSU (*17*), *Rpx* (*14*), POMC, *Pit-1* (*25*), GH (*26*), and βTSH (*27*), according to published procedures (*28*). Sections were stained with Hoechst and simultaneously viewed in dark-field and ultraviolet illumination for photography as described.

tivation of βTSH, PRL, and *Pit-1* promoters in vitro (*9*). Our results establish that *Lhx3* is a general regulator of pituitary-specific gene expression during development in vivo.

In the wild-type mouse, αGSU was expressed in the rostral tip of the pituitary at E12.5 (Fig. 3C) and in cells distributed throughout most of the pituitary at E15.5 (Fig. 3D). αGSU expression was undetectable in the $Lhx3^{-/-}$ embryos at E12.5 or E15.5. Transcripts of βTSH, which is expressed independently of αGSU (*17*), as well as GH, were detected in the wild-type pituitary at E16.5 but not in the $Lhx3^{-/-}$ pouch (Fig. 3, F and G), indicating that the thyrotroph and somatotroph lineages were entirely missing. No LH-positive cells were detected by immunostaining in the residual tissue attached to the bursa of the E18.5$^{-/-}$ pituitary (*12*). However, because of the late activation of LH and the small number of cells expressing LH in the wild-type pouch before birth (*15*), it could not be unequivocally established whether gonadotrophs were entirely missing or were drastically reduced in number.

The specification of the somatotroph, lactotroph, and caudomedial thyrotroph lineages is *Pit-1*–dependent (*7*, *18*). *Pit-1* transcription was not activated in the mutant (Fig. 3E). Accordingly, *Lhx3* not only synergizes with *Pit-1* in regulating downstream gene expression but also is required to activate, directly or indirectly, the *Pit-1* gene itself.

Four of the five lineages of the anterior pituitary—thyrotrophs, gonadotrophs, and *Pit-1*–dependent somatotrophs and lactotrophs—are specifically depleted in the $Lhx3^{-/-}$ mutant, suggesting that *Lhx3* expression is required for the cells of the pituitary primordium to commit to these pituitary-specific lineages. The absolute requirement for *Lhx3* for pituitary organogenesis is reminiscent of the pivotal roles that other transcription factors, such as *SF1*, *Pax-6*, and *IPF-1/pdx-1*, play in the determination of other organs (*13*, *19*). Our data do not indicate whether *Lhx3* functions by regulating genes that are typical of terminal differentiation, as has been shown in vitro (*9*), or by defining a common precursor for the differentiated cell lineages, or both. However, the fact that multiple cell types share a critical transcription factor that is essential for lineage specification, proliferation, and elaboration of marker gene expression argues for a common *Lhx3*-dependent precursor.

Pro-opiomelanocortin (POMC), expressed by the corticotrophs and melanotrophs, is initially activated in the floor of the diencephalon (E10.5) and subsequently in the pituitary (E12 to E13) (*15*, *16*). POMC was detected both in the floor of the diencephalon and in the pituitary in both *Lhx3* mutant and wild-type mice (Fig. 3, H through J), although the domain of expression in the pituitary was drastically reduced in the mutant and confined to a small cohort of cells at the ventral base of the pouch remnant (Fig. 3, I and J). The placement of these cells corresponded roughly to the position of the first presumptive corticotroph cells to differentiate in the wild-type pouch at E13 [see (*6*, *15*, *16*)]. Thus, the specification of the corticotroph cell lineage occurred in the absence of *Lhx3* gene activity, indicating that some cells of the mutant primordium are committed to a pituitary-specific differentiation program. These data also suggest that the derivation of the corticotroph lineage is distinct and that its ontogenic pathway departs from that of the other lineages at a very early stage of pituitary development, perhaps before the derivation of αGSU-expressing progenitor cells. The data also argue that the cells of the early Rathke's pouch are heterogeneous in their developmental potential.

Although some $Lhx3^{-/-}$ pouch cells were able to differentiate and express POMC, a marker for the corticotroph lineage, these cells failed to proliferate. Thus, deficits in proliferation affected all cell types, not just those that did not differentiate. The failure to proliferate could be an intrinsic feature common to all −/− pituitary cells or it could be due to the failure of one or more pituitary cell types to differentiate and produce trophic factors that indirectly affect the proliferation of other neighboring cells. The defect could also result from an inability of the −/− pouch cells to respond to factors produced by the adjacent structures, the hypothalamus or the mesenchyme, which provide proliferative cues to pituitary explants in vitro (*3*, *20*). Finally, the failure to proliferate could result from the inability of the hypothalamus to produce proliferative factors, due to lack of earlier instructive signaling from the pouch.

Many lines of evidence indicate that contact between the floor of the diencephalon (hypothalamus) and Rathke's pouch is critical for proper determination and differentiation of these structures during the early stages of pituitary development (*2*–*5*, *20*). POMC provides the best molecular indicator of these interactions, as it is not activated in the hypothalamus (*3*, *4*) nor in the pituitary primordium (*5*) without contact with the adjacent tissue at the critical time in development. In the $Lhx3^{-/-}$ mutant, a morphologically normal Rathke's pouch was initially formed that expressed *Rpx* and ultimately POMC. The floor of the hypothalamus, including the median eminence and the posterior lobe of the pituitary, appeared to differentiate normally, as judged by gross morphology and by the expression of POMC (Fig. 3H) and vasopressin (*12*). These observations suggest that the mutant pouch is capable of instructive communication with the neuroectoderm during development. Thus, the *Lhx3* mutant mice provide a genetic paradigm for the study of the early development of the pituitary and the ontogeny of the hypothalamic-pituitary axis in mammals.

REFERENCES AND NOTES

1. J. L. Schwind, *Am. J. Anat.* **41**, 295 (1928).
2. S. Diakoku, M. Chikamori, T. Adachi, Y. Maki, *Dev. Biol.* **90**, 198 (1982); W. Etkin, *Neuroendocrinology*, L. Martini and W. F. Ganong, Eds. (Academic Press, New York, 1967), pp. 261–282; R. Ferrand, *Arch. Biol.* **83**, 297 (1972).
3. S. Daikoku *et al.*, *Dev. Biol.* **97**, 81 (1983).
4. S. Kikuyama, H. Inaco, B. G. Jenks, K. Kawamura, *J. Exp. Zool.* **266**, 216 (1993).
5. K. Kawamura and S. Kikuyama, *Cell Tissue Res.* **279**, 233 (1995); Y. G. Watanabe, *ibid.* **227**, 257 (1982).
6. D. M. Simmons *et al.*, *Genes Dev.* **4**, 695 (1990).
7. S. J. Rhodes, G. E. DiMattia, M. G. Rosenfeld, *Curr. Opin. Genet. Dev.* **4**, 709 (1994).
8. N. G. Seidah *et al.*, *DNA Cell Biol.* **13**, 1163 (1994).
9. I. Bach *et al.*, *Proc. Natl. Acad. Sci. U.S.A.* **92**, 2720 (1995).
10. A. B. Zhadanov, S. Bertuzzi, M. Taira, I. B. Dawid, H. Westphal, *Dev. Dyn.* **202**, 354 (1995).
11. M. Taira, W. P. Hayes, H. Otani, I. B. Dawid, *Dev. Biol.* **159**, 245 (1993).
12. H. Z. Sheng *et al.*, data not shown.
13. X. Luo, Y. Ikeda, K. L. Parker, *Cell* **77**, 481 (1994).
14. E. Hermesz, S. Mackem, K. A. Mahon, *Development* **122**, 41 (1996).
15. M. A. Japon, M. Rubinstein, M. J. Low, *J. Histochem. Cytochem.* **42**, 1117 (1994).
16. S. Elkabes, Y. P. Loh, A. Niebuigs, S. Wray, *Dev. Brain Res.* **46**, 85 (1989).
17. S. K. Kendall, L. C. Samuelson, T. L. Saunders, R. I. Wood, S. A. Camper, *Genes Dev.* **9**, 2007 (1995).
18. J.-L. Castrillo, L. E. Theill, M. Karin, *Science* **253**, 197 (1991).
19. R. E. Hill *et al.*, *Nature* **354**, 522 (1991); J. Jonsson, L. Carlsson, T. Edlund, H. Edlund, *ibid.* **371**, 606 (1994); M. F. Offield *et al.*, *Development*, in press.
20. M. Kusakabe, T. Sakakura, M. Sano, Y. Nishizuka, *Dev. Growth Differ.* **26**, 263 (1984).
21. A. B. Zhadanov, N. G. Copeland, D. J. Gilbert, N. A. Jenkins, H. Westphal, *Genomics* **27**, 27 (1995).
22. V. L. J. Tybulewicz, C. E. Crawford, P. K. Jackson, R. T. Bronson, R. C. Mulligan, *Cell* **65**, 1153 (1991).
23. E. Li, T. H. Bestor, R. Jaenisch, *ibid.* **69**, 915 (1992).
24. S. A. Wood, N. D. Allen, J. Rossant, A. Auerbach, A. Nagy, *Nature* **365**, 87 (1993).
25. S. A. Camper, T. L. Saunders, R. W. Katz, R. H. Reeves, *Genomics* **8**, 586 (1991).
26. D. I. H. Linzer and F. Talamantes, *J. Biol. Chem.* **260**, 9574 (1985).
27. W. W. Chin, H. M. Kronenberg, P. C. Dee, P. F. Ma, J. F. Habener, *Proc. Natl. Acad. Sci. U.S.A.* **78**, 5329 (1981).
28. G. W. Robinson, S. Wray, K. A. Mahon, *New Biol.* **3**, 1183 (1991).

29. We thank M. Taira, I. Dawid, S. Camper, and J. Drouin for valuable discussions and suggestions; J. Ward for pathological examination; K. Moriyama for immunohistochemistry; Y.-W. Chu and K. Cveklova for their assistance in genotyping and in situ experiments; and D. Gordon, S. Camper, and Y. P. Loh for the gift of riboprobe plasmids. LH antiserum was obtained from the National Hormone and Pituitary Program, NIDDK.

27 October 1995; accepted 1 February 1996